Total-body 18F-FDG PET Scan in Oncological Patients: How Fast could it be?

Pengcheng Hu (hpc0210@126.com)
Zhongshan Hospital, Fudan University https://orcid.org/0000-0003-3720-3250
Yiqiu Zhang
Zhongshan Hospital Fudan University
Haojun Yu
Zhongshan Hospital Fudan University
Shuguang Chen
Zhongshan Hospital Fudan University
Hui Tan
Zhongshan Hospital Fudan University
Chi Qi
Zhongshan Hospital Fudan University
Yun Dong
United Imaging Healthcare
Ying Wang
United Imaging Healthcare
Zilin Deng
United Imaging Healthcare
Hongcheng Shi
Zhongshan Hospital Fudan University

Research Article

Keywords: total-body PET/CT, digital PET/CT, image quality, protocol optimization

Posted Date: March 19th, 2021

DOI: https://doi.org/10.21203/rs.3.rs-320600/v1

Version of Record: A version of this preprint was published at European Journal of Nuclear Medicine and Molecular Imaging on April 18th, 2021. See the published version at https://doi.org/10.1007/s00259-021-05357-5.

Abstract

Purpose: The aim of the study was to explore a fast PET scan protocol of the total-body uEXPLORER scanner by assessing the image quality consistent to that of a conventional digital PET/CT scanner both from the phantom and clinical perspectives.

Methods: The phantom study using a NEMA/IEC NU-2 body phantom was performed both on a total-body PET/CT (uEXPLORER) and a digital routine PET/CT (uMI 780), with hot sphere to background activity concentration ratio of 4:1. The contrast recovery coefficient (CRC), background variability (BV), recovery coefficient RCmax and RCmean were assessed and compared between that in uEXPLORER with the different scanning duration and reconstruction protocols and that in uMI 780 with clinical settings. The coefficient of variation (COV) of the uMI 780 with clinical settings were calculated and used as a threshold to determine the optimized scanning duration and reconstruction protocols were, which can provide a consistent image quality for the two scanners. And subsequently, the proposed protocol was validated by 30 oncological patients. Images acquired in uMI 780 with a 2-3 minute for each bed position were referred as G780. All PET raw data were reconstructed using data-cutting technique to simulate a 30s, 45s or 60s acquisition duration on uEXPLORER. The iterations were 2 and 3 for uEXPLORER, referred as G30s_3i, G45s_2i, G45s_3i, G60s_2i, and G60s_3i. A 5-point Likert scale was used in the qualitative analysis to assess the image quality. The image quality was also compared with the liver COV, the lesion target-to-background ratio (TBR), and the lesion signal-to-noise ratio (SNR).

Results: In the phantom study, CRC, BV, RCmax and RCmean in uEXPLORER with different scanning duration and reconstruction iterations were compared with that in uMI 780 with clinical settings and a minor fluctuation was found among different scanning durations. COV of the uMI 780 with clinical settings was 11.6% and determined protocol with a 30-45s scanning duration and 2 or 3 iterations to provide a similar image quality.In the quantitative analysis on the clinical images, there was no significant difference between G780 and G45s_3i. All the other groups in uEXPLORER with a 45s- and above acquisition showed a significantly improved image quality than that in uMI 780 with clinical settings. Comparing the liver COV, there was no significantly difference between G780 and G30s_3i. And no significant difference in lesion TBR was identified between G780 and G45s_2i, while uEXPLORER had a better performance in lesion SNR compared to that in uMI 780 with clinical settings.

Conclusions: This study demonstrated a fast PET protocol with a 30-45s acquisition in uEXPLORER with consistent image quality to that in uMI 780 with clinical settings.

Introduction

Positron emission tomography and computed tomography (PET/CT) is an important imaging tool being widely used for diagnosis, staging, restaging, and therapy response assessment in oncology. [1–7] Efforts have been made over the past years to improve PET performance including the implementation of fast scintillator (lutetium oxyorthosilicate, LSO) and solid-state silicon photomultiplier (SiPM), the

introduction of time of flight (TOF) and point spread function (PSF) reconstruction technique, and the extension of the axial field of view (AFOV). [8–16]

The state-of-the-art PET/CT, the total-body PET/CT scanner (uEXPLORER, United Imaging Healthcare, China), implements all the above mentioned improvements with an AFOV up to 194cm. The total-body PET scanner provides a very high sensitivity of 176 kcps/MBq, count-rate performance with a peak noise equivalent count-rate (NECR) of approximately 2 Mcps for total-body imaging, coupled with good spatial resolution capabilities for human imaging (≤ 2.9 mm FWHM near the center of the AFOV). [17] This total-body PET/CT scanner has been used in the clinical practice, together with other routine PET/CT scanners in our site. Obviously, this total-body PET/CT can provide a superior performance than the routine scanners. Benefited from the sensitivity gain, a fast scan protocol is feasible with a shortened PET acquisition by a factor of even up to 40 theoretically. [18] A fast PET scan can improve patient comfort, especially for those who can't bear a routine PET scan with an acquisition of 10–20 minutes. Moreover, a fast PET scan can be applied in other specific scenarios, such as a single breath-hold PET acquisition for lung cancer. However, to what extent the scan acquisition can be shortened with a maintaining image quality to that in the routine practice has not been studied. To the best of our knowledge, such a comparison based on both the phantom and clinical data has not been performed yet. A recently commercially available digital PET/CT (uMI 780, United Imaging Healthcare, China) was selected as a routine PET/CT scanner in the study. It is some-what a "miniature" of the total-body PET/CT with a limited AFOV of 30cm, with the same technique implemented except the extended AFOV. It has a spatial resolution of 2.9 mm, sensitivity of 16.0 cps/kBq, peak NECR activity of 200 kcps and a TOF resolution of 430 ps. [19]

In the first part of the study, utilization of phantom with known geometry and activity preparation was a basic to assess the image quality of the PET scanners. To simulate the patient morphology and tracer distribution, the National Electrical Manufactures Association (NEMA)/International Electrotechnical Commission (IEC) NU-2 phantom has been commonly used in PET studies and also was adopted in this inter-scanner study. [20, 21] We compared background variability (BV), recovery coefficients (RCs), and contrast recovery coefficient (CRC) in uEXPLORER with the different scanning duration and reconstruction protocols to those in the reference uMI 780 protocol as in the our clinical practice. And the coefficient of variation (COV) was used and compared to determine an optimized protocol for a consistent image quality. In the subsequent clinical study, these protocols were validated with an enrolled cohort of oncological patients.

The aim of the study was to explore a fast PET scan protocol of the total-body uEXPLORER scanner by assessing the image quality consistent to that of the uMI 780 digital PET/CT scanner both from the phantom and clinical perspectives.

Methods

Phantom Study

Phantom Preparation

A NEMA/IEC NU-2 phantom was used to describe the small lesion detectability and contrast recovery versus background noise in oncologic ^{18}F-FDG PET/CT images for the two PET/CT scanners in the phantom study. [22] The phantom has six spherical inserts with 10, 13, 17, 22, 28, and 37 mm in diameter. In addition, a 16cm-long cylinder lung insert with a diameter of 5cm was positioned in the center of the phantom to simulate the lung tissue attenuation. To simulate the average hepatic activity concentration in patients who underwent ^{18}F-FDG oncologic PET 60 minutes after a weight-based administration of 3.7 MBq/kg, the phantom was filled with a background activity concentration of 2.65kBq/ml which was ensured at the start of data acquisition. And the radioactivity concentration ratio of the background to all the six spheres was 1:4. [23] The phantom was prepared following the same procedure on a different day for the acquisition on the other PET/CT scanner.

Phantom Acquisition and Reconstruction

The phantom was placed horizontally on the bed to make sure the hot spheres were localized at the center of axial field of view in uMI 780 and the center of Unit 2 in uEXPLORER. Then, a CT scan was executed for attenuation correction followed by an emission scan with 10 minutes in both the scans. Images in uMI 780 were reconstructed with clinical settings. And PET reconstruction was performed with 2-min duration using TOF + PSF, subsets = 20, iteration = 2, image matrix = 150 × 150, FOV = 500, and the full width at half maximum (FWHM) of the Gaussian filter function of 3 mm.

To compare the clinical PET/CT images of uEXPLORER with the routine images in uMI 780 with clinical settings, reconstructions were performed using time subsets of 0.3, 0.5, 0.68, 1, 1.36, 2.04, 2.72, 4.09, 5.46 and 6.38mins from the original 10 minutes data with normalization, system dead time, random, scatter and attenuation correction. Here the reconstruction was performed using TOF + PSF, subsets = 20, iteration = 2 and 3, matrix = 192×192, FOV = 600, and the FWHM of the Gaussian filter function of 3 mm.

Phantom Data Analysis

For each set of the images from the two scanners, three rectangular regions of interests (ROIs), with an area of 900 mm^2, were drawn on the three central transverse image slices (as shown in Fig. 1). The noise was determined by dividing the standard deviation to the mean pixel value for each ROI. And the image coefficient of variation (COV) for a reconstructed image was acquired by averaging the values in the nine ROIs. A COV < 15% was considered as an acceptable noise level as suggested in the EARL procedure. [24]

For spheres characterization, a cubic volume of interest (side of 50 mm) was placed on each sphere of the phantom as shown in Fig. 2. [25]The maximum RCs of all the spheres were obtained as in the EANM Guidelines for tumor PET imaging. [20, 25] And the mean RCs were derived with additional spherical VOIs, matching the actual insert volume. Furthermore, the corresponding contrast recovery coefficients (CRC) were analyzed according to NEMA NU-2 2018 standard. [22]

In this study, the COV, RCs, CRC with a routine 2-min scanning duration in uMI 780 with clinical settings was used as the reference. To compare the image noise with that in the reference, a graph was plotted to compare the COVs with different scanning durations in uEXPLORER. And the optimized scanning duration and reconstruction parameters in uEXPLORER can be determined when the noise was consistent with that in uMI 780 with clinical settings. Then in the subsequent clinical study the reconstructions were performed with the optimized scanning duration and the proposed parameters for uEXPLORER. Compared to that in uMI 780 with clinical settings, the image quality with optimized scanning duration and reconstruction parameters in uEXPLORER can be further validated.

It should be noted that there were different image matrices, FOVs, pixel sizes and iterations used in the image reconstruction both in the phantom and clinical study for the two scanners according to the clinical practice in our site.

Clinical Study

Patients

Forty consecutive patients, referred for cancer staging or restaging in our hospital, were prospectively recruited in the study. In order to minimize the impact induced by the delay time between the two scans, studies with delay time larger than 40 minutes were excluded from the study. In total, ten studies were excluded because of the long delay time and other technical issues (motion artifacts and the difference in the scan order). The enrolled 30 patients (10/20 female/male, age 64.2 ± 9.3 years) were diagnosed with lung cancer (n = 3), gastric cancer (n = 5), esophageal cancer (n = 3), hepatocellular carcinoma (n = 1), bile duct cancer (n = 1), duodenal cancer (n = 1), pancreatic cancer (n = 2), colon cancer (n = 5) and rectal cancer (n = 7). The demographic and clinical characteristics of the enrolled patients were listed in Table 1.

Table 1
Patient demographic and clinical information

Characteristic	Data
Age (years)	64.2 ± 9.3[37, 79]*
Sex(Female/Male)	10/20
Weight (kg)	62.9 ± 9.5[40.8, 78.1]*
Height (cm)	163.7 ± 8.0[148.0, 183.1]*
BMI(kg/m^2)	23.4 ± 2.9[18.1, 30.4]
Injected dose (MBq)	227.9 ± 34.9[149.5, 289.7]*
Injected dose per weight (MBq/kg)	3.62 ± 0.17[3.34, 3.95]*
Uptake time of uMI 780 in uMI780-first group (min)	72 ± 15[53, 104]*
Uptake time of uEXPLORER in uMI780-first group (min)	98 ± 17[76, 103] *
Uptake time of uMI 780 in uMI780-second group (min)	87 ± 20[60, 129]*
Uptake time of uEXPLORER in uMI780-first group (min)	67 ± 18[40, 104] *
Delayed time between two PET scans (min)	24 ± 28[10, 39]*
Location of the primary lesion	3^+
Lung	3^+
Esophagus	3^+
Liver	5^+
Stomach	2^+
Pancreas	1^+
Bile duct	1^+
Duodenum	5^+
Colon	7^+
Rectum	
*Data were presented as mean ± SD [range].	
$^+$ indicated the number of the patients.	

The study was approved by the Institutional Review Board of Shanghai Zhongshan Hospital affiliated to Fudan University, and a written consent form was signed prior to the scan.

Clinical PET/CT Imaging and Reconstruction

All patients have fasted for at least 6 hours before the injection of ^{18}F-FDG. The blood glucose levels of patients was under 11 mmol/L before the injection. After a single radiotracer injection of ^{18}F-FDG (3.7 MBq/kg), all patients underwent two PET/CT scans, on a digital PET/CT scanner (uMI 780, United Imaging Healthcare, China) and a total-body PET/CT scanner (uEXPLORER, United Imaging Healthcare, China). With an uptake of approximate 60 minutes after the injection, 15 patients were initially scanned with uEXPLORER and underwent a sequent scan with uMI 780. In the remaining 15 patients, the scans were performed with an alternative order. The uptake time was 84 ± 23 minutes for uEXPLORER, and 79 ± 19 minutes for uMI 780. Time delay between two scans were controlled under 40 minutes with a mean value of 24 ± 8 minutes.

Both of the CT subsystems consist of a 160-slice detector. A diagnostic CT was performed in the first scan with 120 kVp, tube current modulation, and spiral pitch factor of 0.9875, slice thickness of 1 mm and slice increment of 1 mm. No intravenous or oral contrast was used. And a low-dose CT acquisition (120 kVp, 9 mAs, spiral pitch factor of 1.10125, 1.4 mm slice thickness with slice increment of 3.0 mm) for attenuation correction was used in the second scan in order to minimize the radiation exposure to the patients.

As in our clinical practice, PET was acquired in uMI 780 with a 2–3 minute for each bed position covering the lung, abdomen and pelvic region. The total PET acquisition was about 10–13 minutes for the body part with an additional 3minutes for the head. In uEXPLORER, PET was acquired in one bed position to cover the entire patient body with a total acquisition time of 5 minutes in the study. All PET raw data were stored in list mode, and the reconstruction were performed using data-cutting technique to simulate a 30s, 45s or 60s acquisition duration on uEXPLORER. Both the reconstruction were performed with the following parameters as determined in the phantom study: a FOV of 600, a matrix of 192×192, 20 subsets and the FWHM of the Gaussian filter function of 3 mm. The iterations were 2 and 3 for uEXPLORER, referred as G30s_3i, G45s_2i, G45s_3i, G60s_2i, and G60s_3i. The standard corrections, including decay, random, dead time, attenuation and normalization correction, were applied in the all PET reconstructions. In addition, the point-spread-function (PSF) and time-of-flight (TOF) were also used to reconstruct the images. However, due to the system configuration, the slice thickness was slightly different, as in the phantom study.

Clinical Image Analysis

The image quality was qualitatively assessed by two experienced nuclear medicine physicians with over 10-year experience in interpreting PET/CT images on a dedicated workstation (uWI, United Imaging Healthcare, China). A 5-point Likert scale was used to score the overall image quality with 1 = unacceptable image quality for diagnosis, 2 = acceptable image quality with no need to repeat the scan,

3 = fair image quality as in the routine practice, 4 = good image quality with performance excessed the routine practice and 5 = excellent image quality (as shown in Fig. 2).

The PET image was then assessed by a technician supervised by an experienced nuclear medicine physician. For PET images of each patient, a circular region of interest (ROI) with a diameter of 20 ± 2mm were manually drawn in the homogeneous region of the liver far from the edges and lesions. And SUVmax, SUVmean, and SD were measured and recorded. Liver COV was obtained by the following equation, and used as a measure of the image noise (Eq. 1).

$$\mathrm{COV} = \frac{liverSD}{liverSUV_{mean}} \qquad \text{Eq. 1}$$

For each patient, the lesions with a diameter less than 40mm were selected in the study according to the sphere size in the phantom study. For each patient, two lesions (if there were) were selected in < 10mm, 10-20mm, and 20-40mm group, respectively. The lesion uptake was measured by drawing a volume of interest (VOI) with a threshold of 50% of the SUVmax value within the contour margin. Both SUVmax and SUVmean of the lesion were measured. And the target-to-background ratio (TBR) and signal-to-noise ratio (SNR) were calculated by the following equations and was used as a measure of lesion contrast (Eq. 2 & Eq. 3).

$$\mathrm{TBR} = \frac{lesionSUV_{max}}{liverSUV_{mean}} \qquad \text{Eq. 2}$$

$$\mathrm{SNR} = \frac{lesionSUV_{mean} - liverSUV_{mean}}{liverSD} \qquad \text{Eq. 3}$$

Statistical Analysis

Continuous parameters were presented as mean and standard deviation. Cohen's kappa test was used to compare the inter-reader agreement and Wilcoxon signed rank test was used to compare the subjective scores between the uEXPLORER groups and G780 group. The delay time between the two scan orders was compared with independent t test. And paired *t* test was performed to compare the quantitative parameters between the two scanners.

A p value of < 0.05 was considered significant. Statistical analysis was performed with SPSS Version 25.0.

Results

NEMA/IEC body phantom study

Figure 3 showed the transaxial views across the equatorial plane of the various spheres of the phantom, with a scanning duration of 0.3, 0.5, 0.68, 1.0 and 1.5mins in uEXPLORER. It should be emphasized here that the same dose calibrator and isotopes phantom were used in daily quality control for the two PET/CT scanners. And the system cross-calibration in background SUV was within the range of 0.95–1.05.

The measured COV as a function of the scanning duration for uEXPLORER was reported in Fig. 4, where the dashed black line indicated a COV of 11.6% in uMI 780 with clinical settings. As expected, image noise decreased with the increased scanning duration and the increased number of iterations. By a power-law fitting with the COV and scanning duration, the minimal scanning duration was found to be about 30s for uEXPLORER, where the background variability was similar to that in uMI 780 with clinical settings.

Figure 5 and Fig. 6 gave the CRC, RCs, and background variability check for the clinical scanning and reconstruction protocol in uMI 780 and the optimized scanning and reconstruction protocols in uEXPLORER. It showed that CRC had a minor fluctuation among the images with a scanning duration of 30, 45 and 60s. Both CRC and BV increased with the increased number of iterative reconstruction. For all the spheres, uEXPLORER gave a little higher CRC for all the time frame than uMI 780 for both iteration of 2 and 3. The RCmax and RCmean for all the spheres in both the PET/CT scanners were almost within the EARL limits. Table 2 gave the optimized scanning and reconstruction protocols in uEXPLORER which had similar image quality with that in uMI 780.

Table 2
the optimized reconstruction protocol with uMI 780 and uEXPLORER

	uMI780	**uEXPLORER**
Scanning duration/ bed (mins)	2	0.5/0.75 / 1
Reconstruction	OSEM + TOF + PSF	OSEM + TOF + PSF
Subsets	20	20
FOV/Matrix	500 / 150 × 150	600 / 192 × 192
Slice thickness (mm)	1.34	1.443
Iteration	2	2 / 3

Clinical validation

The overall inter-reader agreement of the image quality showed a kappa of 0.875, indicating an almost perfect agreement between the readers. The average scores of the two readers for the protocols were listed in Table 3. The subjective score in G780 was significantly higher than that in G30s_3i ($p = 0.001$) and slightly lower than that in G45s_3i ($p = 0.18$). The other groups in uEXPLORER with a 45s- and above acquisition showed a significant higher score than that in uMI 780.

Table 3
Subjective score in different groups

Group	Subjective score
G780	2.95 ± 0.22
G30s_3i	2.80 ± 0.40*
G45s_2i	3.19 ± 0.55*
G45s_3i	3.03 ± 0.50
G60s_2i	3.28 ± 0.48*
G60s_3i	3.20 ± 0.54*
* indicated a significant difference compared to uMI 780.	

In the semiquantitative analysis, the delay time between the two scans in the two orders was not significantly different ($p = 0.054$) with a mean value of 26 ± 7 min and 21 ± 8min. And thus, the difference due to the delay time can be eliminated. There was no significant difference in COV between G30s_3i and G780 ($p = 0.162$), indicating a consistent image noise in the liver. And all the other groups showed a significantly lower COV value than G780 ($p < 0.001$, as shown in Fig. 7). The groups with a longer acquisition showed a lower COV value, and illustrated a better image noise in these groups. According to the OSEM algorithm characteristics, the image noise increased as the iteration increased for the groups with the same acquisition. However, all the groups presented a COV value less than 15%, indicating a preferred image noise in the clinical routine (as shown in Fig. 8).

A total of 33 lesions were analyzed in the study. For the lesions, there was no significant difference in TBR between G45s_2i and G780 ($p = 0.072$), indicating a consistent lesion conspicuousness (Fig. 9). As shown in Fig. 10, the two reconstructed images resulted in minor visual variations in lesion contrast. And all the other groups showed a significantly higher TBR value than G780 ($p < 0.001$). In addition, all the groups in uEXPLORER showed a larger SNR value than that in G780 group ($p < 0.001$, as shown in Fig. 9).

Discussion

With the advent of the uEXPLORER scanner, the PET/CT scan has evolved to a total-body imaging in clinics. And its superior performance has made it a powerful tool in oncological applications. [18–19, 27–28] The ultra-high sensitivity provides the feasibility of a fast PET scan in routine practice for an improvement of patient comfort and an increased throughput. This study assessed the image quality from the phantom and clinical perspectives to explore a fast PET scan protocol with consistent image quality to that in a routine digital PET scanner. The PET acquisition using a routine PET/CT scanner in a step-and-shoot mode takes about 10–20 minutes for the body part and an additional ~ 3 minutes for the head to cover the scan range from the skull to the mid-thigh. However, in the total-body PET/CT scanner with an AFOV of 194cm, the PET acquisition can be performed with only one bed position to cover the entire patient body. The study demonstrated a fast PET scan with 30–45 seconds acquisition can provide

comparable image quality according to the phantom study and the intra-individual comparison in 30 oncological patients. Furthermore, the study can be regarded as a methodology for an inter-scanner comparison, even for a multi-center study. As known, PET/CT plays an important role in timely monitoring of the therapeutic responses in various diseases, such as lymphoma, where multiple PET/CT scans are needed. [4] Multiple PET/CT scans for a certain patient in the inter-scanner studies always require a consistent image quality to improve the accuracy of the assessment. Therefore, the standardization and optimization of ^{18}F-FDG protocols are essential in inter-scanner studies as illustrated in the study.

In this study, phantom-based study was performed with a standard NEMA/IEC NU-2 phantom. The phantom was selected since it is a simulation of the patient's morphology and tracer distribution and commonly used in the image quality assessment of PET studies. However, in whole-body or total-body PET studies, the scan range of the patients, either from the skull to the mid-thigh or from the skull to the feet, were much larger than the phantom height. And for the total-body PET scans with uEXPLORER, the patient's body were scanned with different parts of the PET detector along the AFOV. During the design of the phantom study, the limited axial coverage of this phantom has been considered. Thanks to the consistent sensitivity of the PET scanners along the AFOV of uEXPLORER [17], the image quality of the patient body can be regarded uniform. Therefore, the standard NEMA/IEC NU-2 phantom was used to assess the image quality in the total-body PET studies.

In the clinical part, the patients were randomly enrolled in the study without strict exclusion criteria, such as age, preparation during the uptake, diabetes, patient size, and cancer type. The enrolled patients group can be regarded as an epitome of the clinical practice. The enrolled patients in the study included almost all the common cancer types where the lesion uptake SUVmax varying from 1.0 to 40. The body mass index (BMI), known as an impact factor on the image quality [29, 30], of the enrolled patients varied in a large range (from 18.1 to 30.4). In addition, they were found to have accompanying diseases other than cancer, such as liver cirrhosis, ascites or with complication of systemic inflammation. And thus, the results of the study indicated a high compatibility and feasibility in the clinical practice.

Furthermore, the reference protocol in uMI 780 was a typical clinical protocol used in our hospital, with a compromise of the image quality and patient throughput. Although not optimal, the protocols obtained in the study can provide image quality as that in routine oncological studies. Based on the results in the qualitative and quantitative analysis, this study proposed a protocol using a 30s-45s acquisition on uEXPLORER with a consistent image quality to that on uMI 780. The phantom and clinical study showed slightly different results. It is well understood that the phantom study can just simulate the patient morphology and tracer distribution in a simplified way. In the phantom study, the tracer were uniformly distributed in the background and in each hot sphere. However, the tracer distribution in patients was totally different, and with more complexity. The patient related factors, such as body weight, blood glucose level, and liver cirrhosis, can impact the tracer distribution. And thus, a phantom with more anthropomorphic structures and different administered activity will be considered in future studies. Other factors may also impact the results of the clinical study. Due to the different reconstruction slice thickness, it was sometimes difficult to find the same slice between the uEXPLORER and uMI 780 images.

The variation between two consecutive slices can induce a bias of the results. In future studies, it can be improved by using an average of several consecutive slices to minimize such bias or drawing a volume of interest (VOI) instead of ROI.

Our study had several limitations. The scans are always performed in a step-and-shoot mode with multiple bed positions with some overlap in a whole-body PET acquisition, whereas the total-body PET acquisition are performed with one bed position to cover the entire patient body. However, in the phantom study, we simplified the acquisition protocol using one bed position for both the scanners. In addition, we only assessed the image quality of the patient body, and assessment on patient head was beyond the scope of the study. Due to the intrinsic limitation of the phantom study, it was difficult to study patients with diversities. Furthermore, the lesions selected in the clinical study were all less than 40mm in diameter according to the sphere size in the phantom study, which may lead a bias on the results.

Conclusion

This study demonstrated a fast PET protocol with a 30-45s acquisition and standard OSEM algorithm on uEXPLORER can provide consistent image quality to that in uMI 780 with clinical settings. Besides, it provides a methodology for a standardization and comparison on the image quality to promote the inter-scanner study.

Declarations

Funding

This study is supported by Shanghai Municipal Key Clinical Specialty Project (shslczdzk03401), Clinical Research Plan of SHDC (SHDC2020CR3079B), Science and Technology Committee of Shanghai Municipality(20DZ2201800), Special Fund for Clinical Research of Zhongshan Hospital, Fudan University(2020ZSLC63), The Youth Medical Talents-Medical Imaging Practitioner Program of Shanghai “Rising Stars of Medical Talent” Youth Development Program(SHWRS[2020]_087)

Conflicts of interest

The authors declare that they have no conflicts of interest.

Availability of data and material

The data that support the findings of this study are available from the corresponding author upon reasonable request.

Authors’ contributions

Pengcheng Hu and Yiqiu Zhang were involved in the study design, data analysis and manuscript preparation. Hui Tan, Chi Qi, and Ying Wang helped with data processing. Haojun Yu, Yusen Gu, and Shuguang Chen helped with image acquisition and processing. Yun Dong and Zilin Deng were in charge of the preparation of the NEMA phantom and of the acquisition. Hongcheng Shi designed the study and contributed to the data analysis and writing of the manuscript. All authors discussed the results and commented on the manuscript.

Ethical approval

All procedures performed in studies involving human participants were in accordance with the ethical standards of the institutional and/or national research committee and with the 1964 Helsinki declaration and its later amendments or comparable ethical standards.

References

1. Boellaard R, Delgado-Bolton R, Oyen WJ, et al. FDG PET/CT: EANM procedure guidelines for tumour imaging: version 2.0. Eur J Nucl Med Mol Imaging. 2015;42(2):328–54.
2. Fletcher JW, Djulbegovic B, Soares HP, et al. Recommendations on the use of 18F-FDG PET in oncology. J Nucl Med. 2008;49(3):480–508.
3. Avril NE, Weber WA. Monitoring response to treatment in patients utilizing PET. Radiol Clin North Am. 2005;43(1):189–204.
4. Juweid ME, Stroobants S, Hoekstra OS, et al. Use of positron emission tomography for response assessment of lymphoma: consensus of the Imaging Subcommittee of International Harmonization Project in Lymphoma. J Clin Oncol. 2007;25(5):571–8.
5. Volpi S, Ali JM, Tasker A, Peryt A, Aresu G, Coonar AS. The role of positron emission tomography in the diagnosis, staging and response assessment of non-small cell lung cancer. Ann Transl Med. 2018;6(5):95.
6. Weber WA. Use of PET for monitoring cancer therapy and for predicting outcome. J Nucl Med. 2005;46(6):983–95.
7. Czernin J, Allen-Auerbach M, Nathanson D, Herrmann K. PET/CT in Oncology: Current Status and Perspectives. Curr Radiol Rep. 2013;1(3):177–90.
8. Akamatsu G, Ishikawa K, Mitsumoto K, et al. Improvement in PET/CT image quality with a combination of point-spread function and time-of-flight in relation to reconstruction parameters. J Nucl Med. 2012;53(11):1716–22.
9. Tong S, Alessio AM, Kinahan PE. Noise and signal properties in PSF-based fully 3D PET image reconstruction: an experimental evaluation. Phys Med Biol. 2010;55:1453–73.
10. Surti S, Karp JS, Popescu LM, Daube-Witherspoon ME, Werner M. Investigation of time-of-flight benefit for fully 3-D PET. IEEE Trans Med Imaging. 2006;25:529–38.

11. Buzhan P, Dolgoshein B, Filatov LA, et al. Silicon photomultiplier and its possible applications. Nuclear Instruments & Methods in Physics Research Section A-accelerators Spectrometers Detectors and Associated Equipment. 2003;504(1):48–52.
12. Rausch I, Ruiz A, Valverde-Pascual I, Cal-González J, Beyer T, Carrio I. Performance Evaluation of the Vereos PET/CT System According to the NEMA NU2-2012 Standard. J Nucl Med. 2019;60(4):561–7.
13. Hsu DFC, Ilan E, Peterson WT, Uribe J, Lubberink M, Levin CS. Studies of a next-generation silicon-photomultiplier–based time-of-flight PET/CT system. J Nucl Med. 2017;58:1511–8.
14. Van Sluis J, De Jong J, Schaar J, et al. Performance characteristics of the digital Biograph Vision PET/CT system. J Nucl Med. 2019;60:1031–6.
15. Chen S, Hu P, Gu Y, Yu H, Shi H. Performance characteristics of the digital uMI550 PET/CT system according to the NEMA NU2-2018 standard. EJNMMI Phys. 2020;7(1):43.
16. Surti S, Karp JS. Impact of detector design on imaging performance of a long axial field of-view, whole-body PET scanner. Phys Med Biol. 2015;60:5343–58.
17. Spencer BA, Berg E, Schmall JP, et al. Performance evaluation of the uEXPLORER Total-body PET/CT scanner based on NEMA NU 2-2018 with additional tests to characterize long axial field-of-view PET scanners. J Nucl Med. 2020 ;jnumed.120.250597.
18. Cherry SR, Jones T, Karp JS, Qi J, Moses WW, Badawi RD. Total-body PET: maximizing sensitivity to create new opportunities for clinical research and patient care. J Nucl Med. 2018;59:3–12.
19. Tan H, Sui X, Yin H, et al. Total-body PET/CT using half-dose FDG and compared with conventional PET/CT using full-dose FDG in lung cancer [published online ahead of print, 2020 Nov 27]. Eur J Nucl Med Mol Imaging. 2020.
20. Panetta JV, Daube-Witherspoon ME, Karp JS. Validation of phantom-based harmonization for patient harmonization. Med Phys. 2017;44(7):3534–44.
21. Gnesin S, Kieffer C, Zeimpekis K, et al. Phantom-based image quality assessment of clinical 18F-FDG protocols in digital PET/CT and comparison to conventional PMT-based PET/CT. EJNMMI Phys. 2020;7(1):1.
22. NEMA standards publication NU. 2-2018 – performance measurements of positron emission tomographs (PET). Rosslyn: National Electrical Manufacturers Association; 2018.
23. Fukukita H, Senda M, Terauchi T, et al. Japanese guideline for the oncology FDG-PET/CT data acquisition protocol: synopsis of Version 1.0. Ann Nucl Med. 2010;24(4):325–34.
24. Boellaard R, Willemsen a T, Arends B, Visser EP. EARL procedure for assessing PET/CT system specific patient FDG activity preparations for quantitative FDG PET/CT studies. 2013; p. 1–3.
25. Koopman D, van Osch JA, Jager PL, et al. Technical note: how to determine the FDG activity for tumour PET imaging that satisfies European guidelines. EJNMMI Phys. 2016;3(1):22.
26. website. EE. Available from: http://earl.eanm.org/cms/website.php?id=/en/projects/fdg_pet_ct_accreditation/accreditation_specifications.htm.

27. Badawi RD, Shi H, Hu P, et al. First Human Imaging Studies with the EXPLORER Total-Body PET Scanner. J Nucl Med. 2019;60(3):299–303.
28. Zhang YQ, Hu PC, Wu RZ, et al. The image quality, lesion detectability, and acquisition time of 18F-FDG total-body PET/CT in oncological patients. Eur J Nucl Med Mol Imaging. 2020;47(11):2507–15.
29. de Groot EH, Post N, Boellaard R, Wagenaar NR, Willemsen AT, van Dalen JA. Optimized dose regimen for whole-body FDG-PET imaging. EJNMMI Res. 2013;3(1):63.
30. Sánchez-Jurado R, Devis M, Sanz R, Aguilar JE, del Puig Cózar M, Ferrer-Rebolleda J. Whole-body PET/CT studies with lowered ¹â¸F-FDG doses: the influence of body mass index in dose reduction. J Nucl Med Technol. 2014;42(1):62–7.

Figures

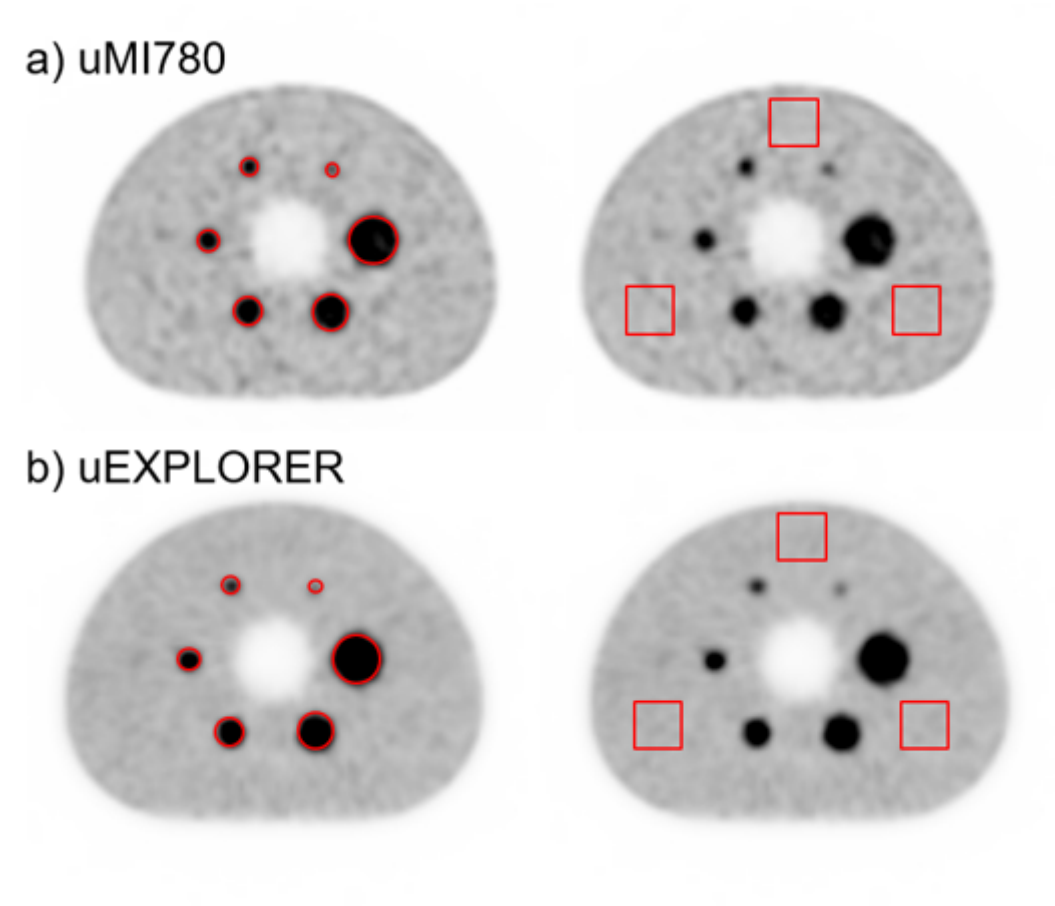

Figure 1

ROI locations for CRC and COV analysis

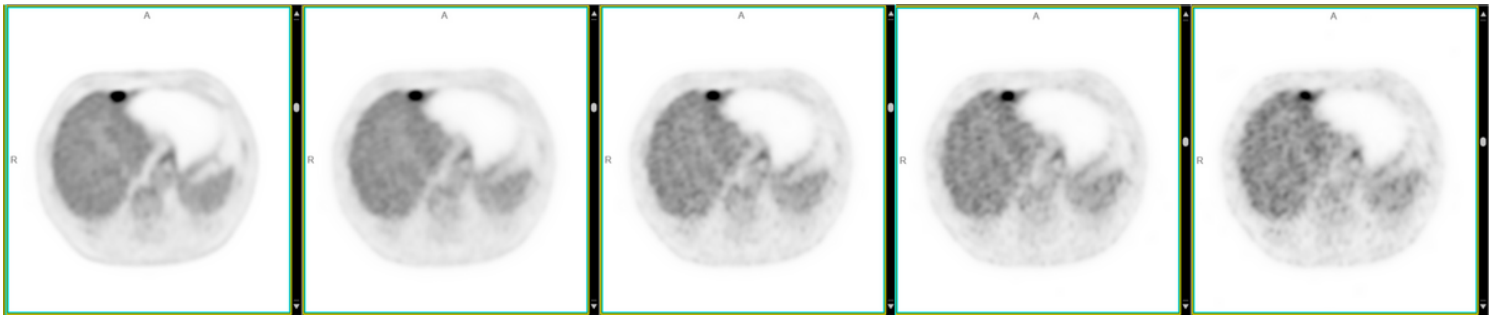

Figure 2

the illustration of the 5-point Likert score for qualitative assessment on image quality (5 to 1 from the left to the right)

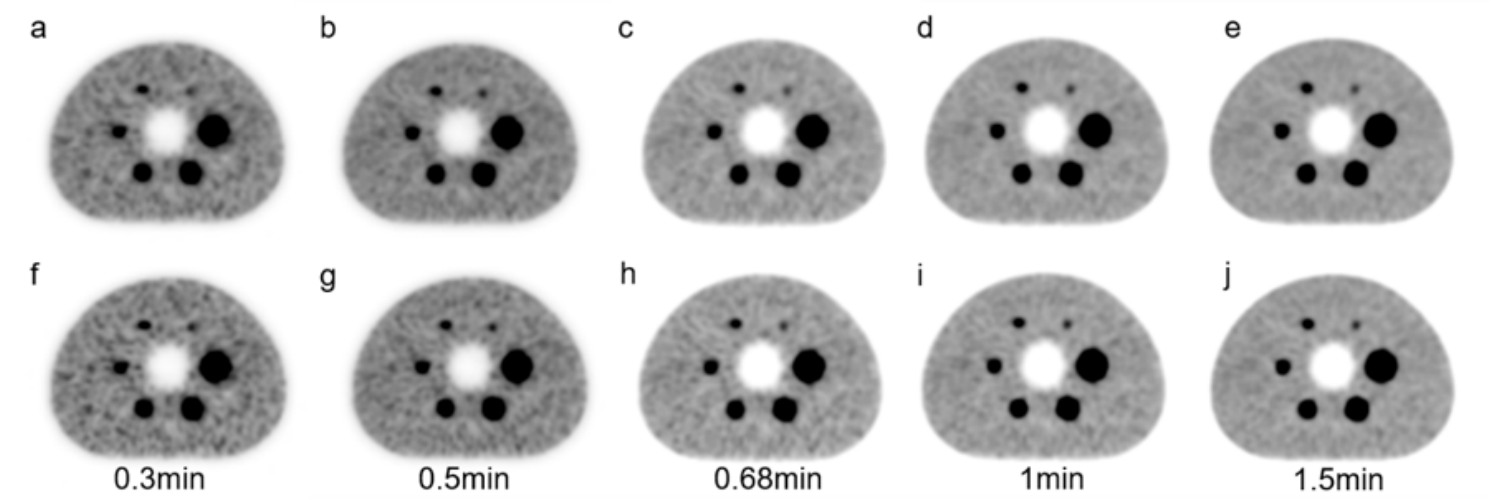

Figure 3

uEXPLORER reconstruction images comparison between iteration =2 and iteration=3 with different duration time: a-e with iteration=2, f-j with iteration=3

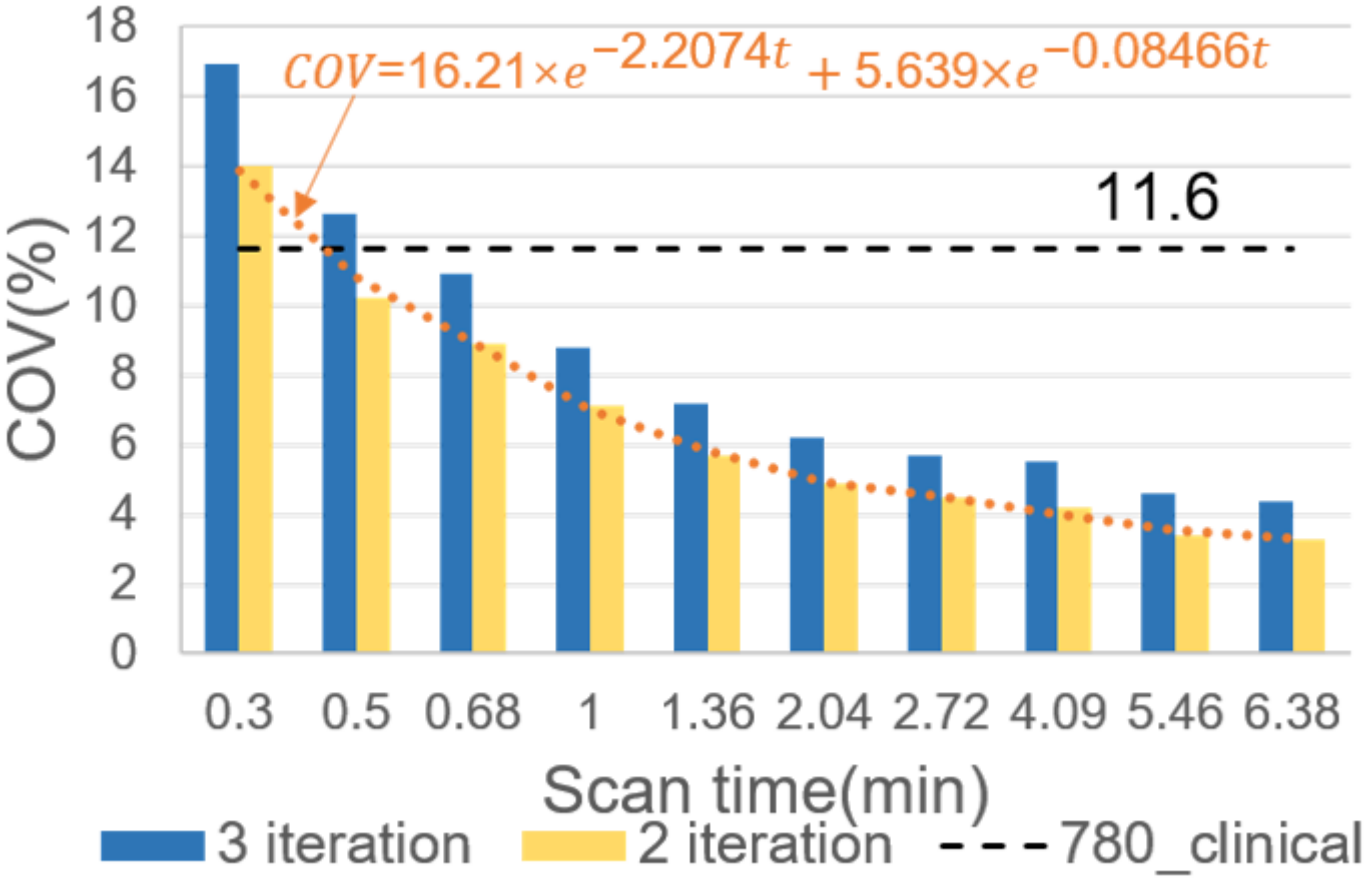

Figure 4

COV of uEXPLORER with different scanning durations

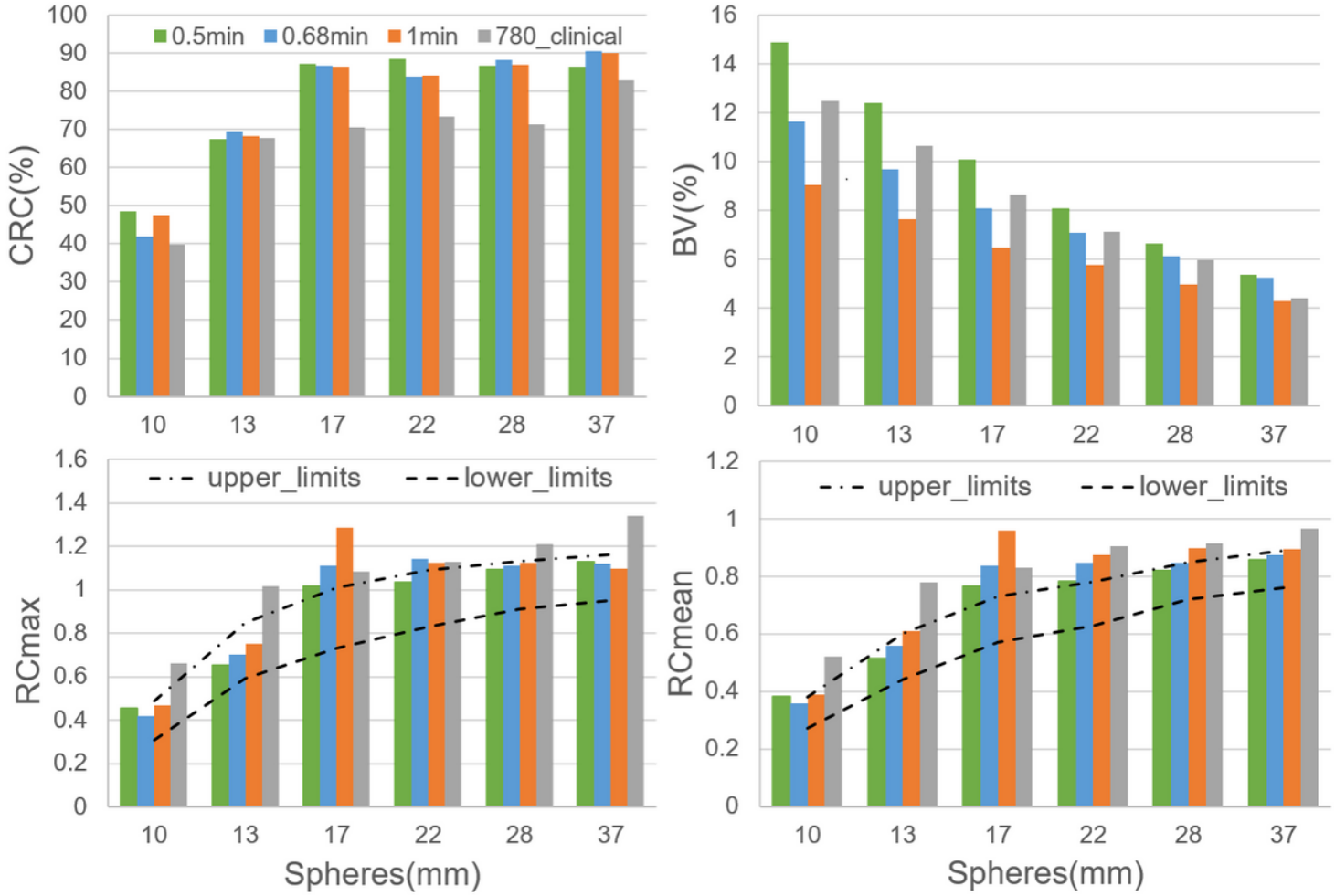

Figure 5

uEXPLORER compared to uMI 780 clinical protocol with 2 iterations

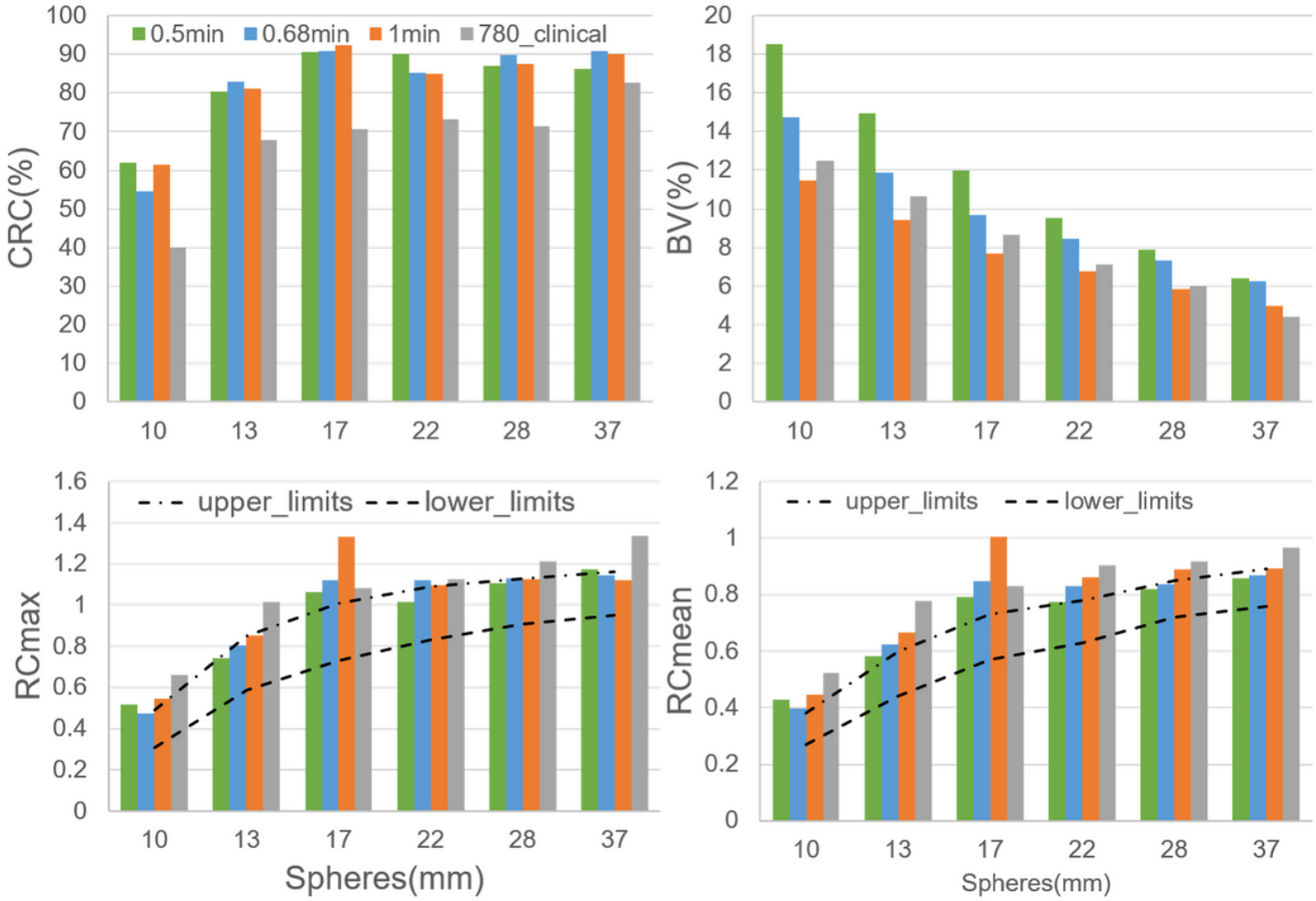

Figure 6

uEXPLORER compared to uMI 780 clinical protocol with 3 iterations

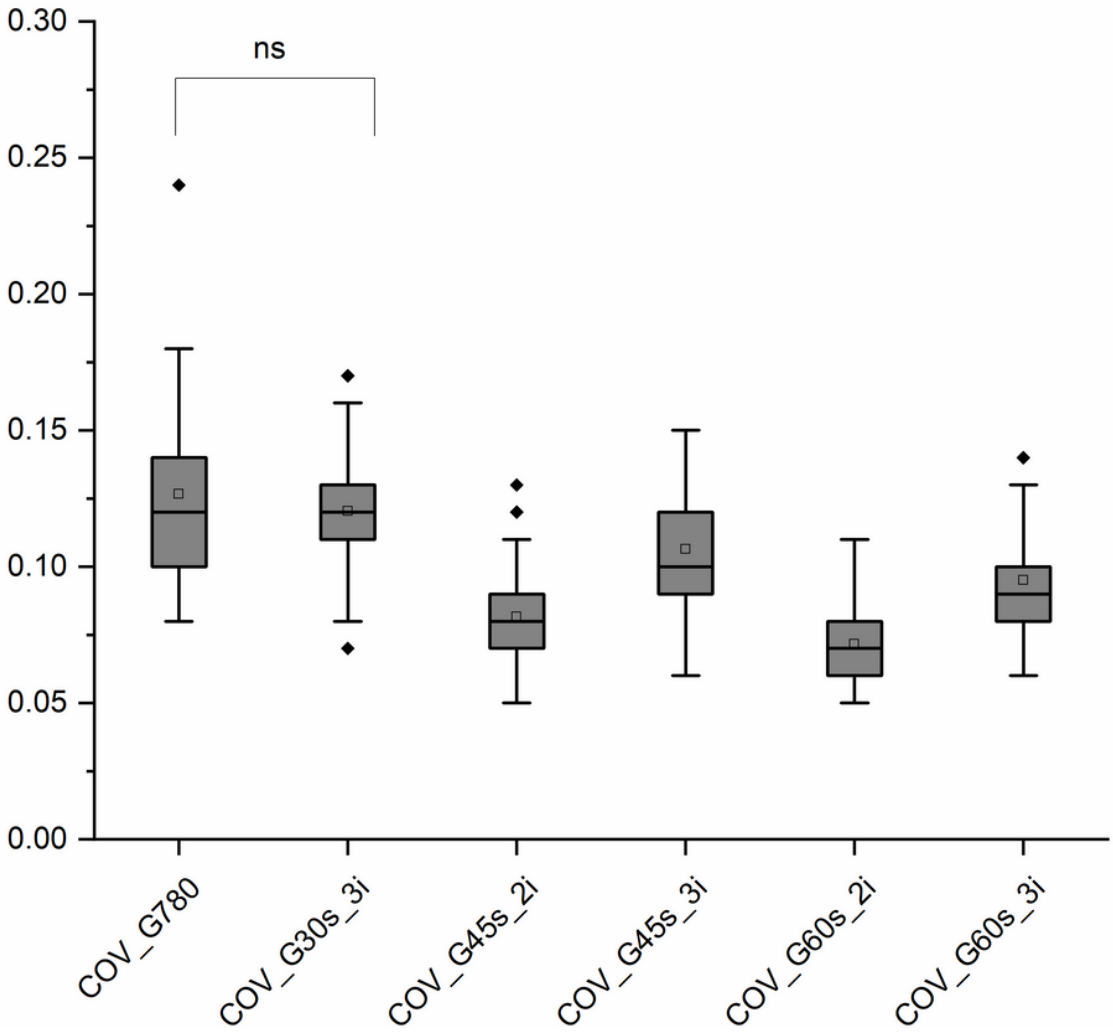

Figure 7

COV comparison between groups in uEXPLORER and uMI 780. There was no significant difference between G30s_3i and G780. A significant lower COV value was found in 45s- and above groups than that in G780 group ($p<0.001$). Here, ns indicates no significant difference.

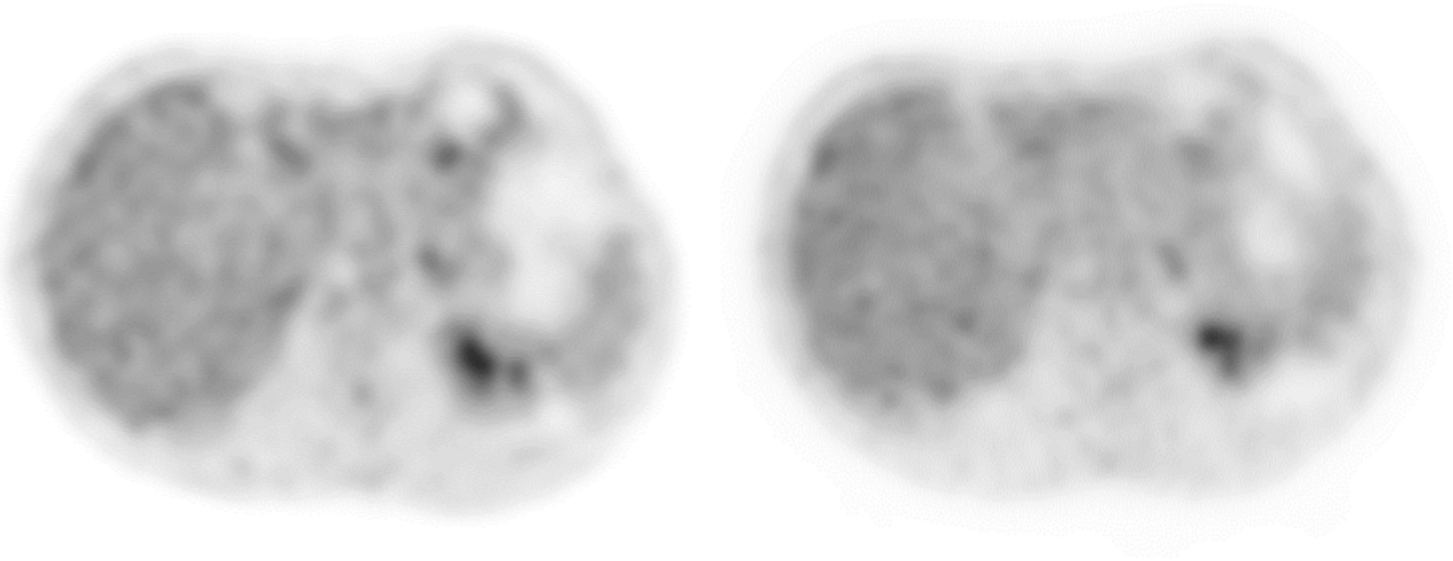

Figure 8

transverse PET images for a 73-year-old female underwent a total-body PET/CT (right) and a subsequent whole PET/CT examination (left). The left PET image was reconstructed with the clinical parameters with an acquisition of 3 minutes, while the right PET image was reconstructed with 3 iterations and an acquisition of 30s. Both the images showed a preferred image noise in clinics.

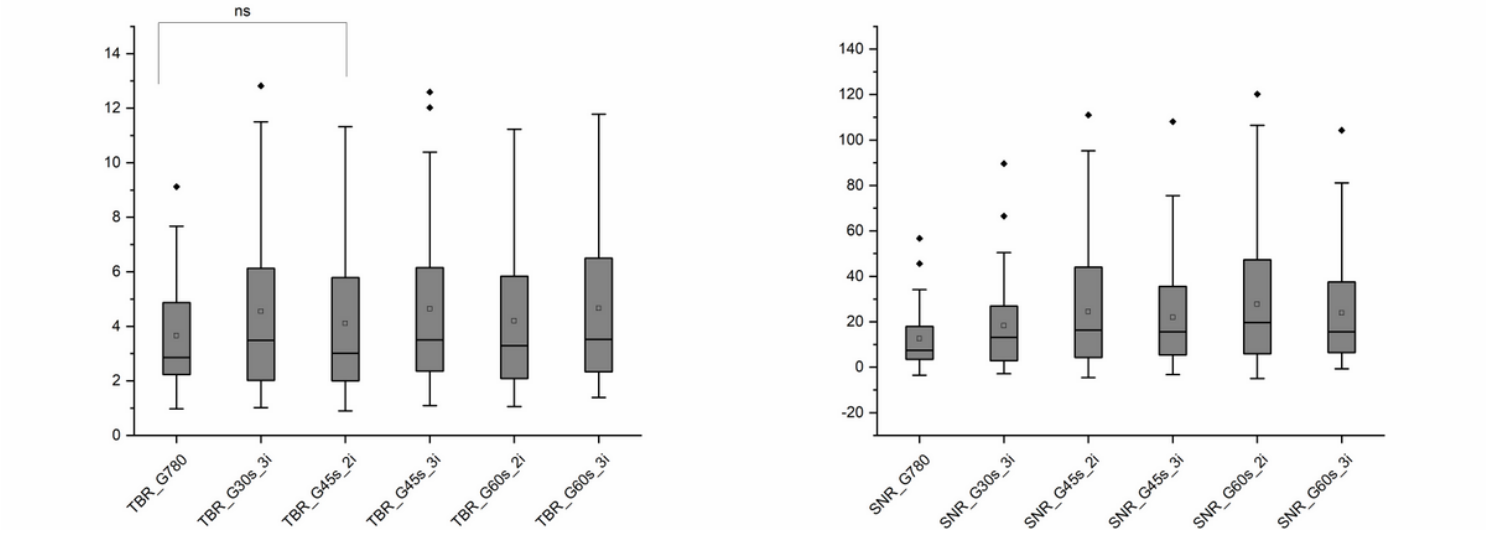

Figure 9

TBR and SNR comparison between groups in uEXPLORER and uMI 780. There was no significant difference in lesion TBR between G45s_2i and G780. A significant higher TBR value was found in other groups of uEXPLORER than that in G780 group (left, $p<0.001$). All the groups in uEXPLORER showed a significant higher SNR than that in G780 group (right, $p<0.001$). TBR=target-to-background ratio; ns=no significant difference

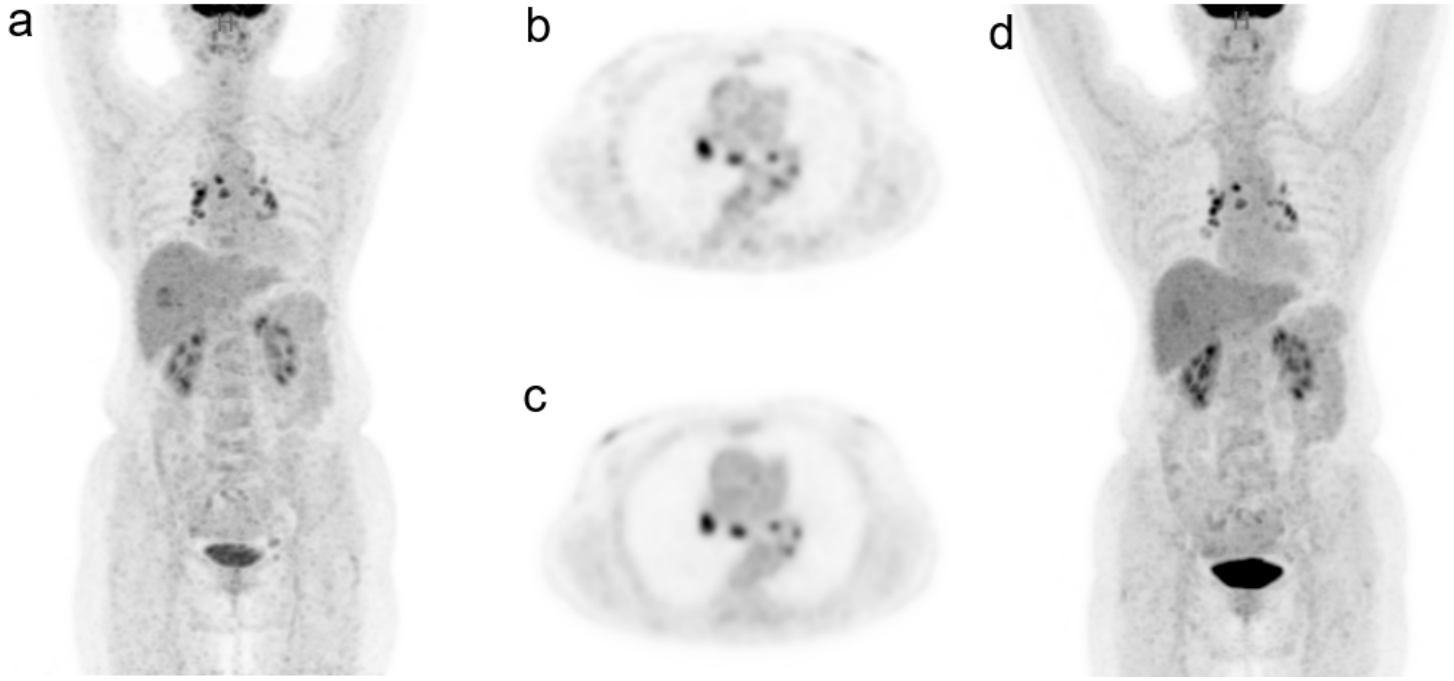

Figure 10

PET images for a 54-year-old female diagnosed with HCC. A total-body PET/CT imaging was performed first (C&D) with a subsequent whole-body PET/CT (a&b). Figure A&B was reconstructed with the clinical parameters with an acquisition of 120s in this bed position, while Figure c&d was reconstructed with 2 iterations and a 45s-acquisition. Both the images showed a fairly good lesion contrast in the clinical practice.